

RESEARCH ARTICLE

## AlPO<sub>4</sub>-C Composite Coating on Ni-based Super Alloy Substrates for High Emissivity Applications : Experimentation on Dip Coating and Spray Coating

Subir Roy\*, S. Rangaswamy Reddy, P. Sindhuja, Dipak Das, and V.V. Bhauprasad

\*Defence Metallurgical Research Laboratory, Hyderabad - 500 058, India

\*E-mail: r\_subir@yahoo.com

### ABSTRACT

High emissivity coating was developed on Ni-based super alloy substrates by dip coating and spray coating techniques using a chemical precursor sol. The coating material was characterised thoroughly by XRD, SEM, TEM and XPS analyses. Characterisation results showed the presence of nano carbon in the AlPO<sub>4</sub> matrix which imparted high emissivity to the coating. Emissivity of the coating varied from 0.6 to 0.9 in the wave length range: 2 μm - 25 μm depending on the thickness of the multilayered coating. Spray coating was very effective for coating of the bigger substrates and TPS panels. Emissivity offered by the spray coated substrates was little lower compared to the dip coated substrates. Cyclic oxidation performances of the coated substrates at 800 °C and 1000 °C for 100 hrs of thermal exposure were recorded and compared with that of the bare substrate. The emissivity coating was found to offer substantial oxidation resistance to the base substrates at high temperatures.

**Keywords:** High emissivity coating, C-263 alloy substrate, oxidation resistance, dip coating, spray coating

### 1. INTRODUCTION

The emissivity of a material (usually denoted as  $\epsilon$  or  $e$ ) is the relative ability of its surface to emit energy by radiation. When heat radiation falls on a body, it is partially reflected, partially transmitted and partially absorbed by the body. If the fraction of energy reflected, transmitted and absorbed are R, T and A respectively, then following the principle of conservation of energy,  $A+R+T=1$ . A blackbody completely absorbs all radiation incidents upon it, and at the same time it emits all the energy that it absorbs with the same absorbing spectrum. Thus its emissivity is equal to 1. Higher emissivity corresponds to an increase in thermal efficiency. Thermal protection systems (TPS) is an integral part in hypersonic and reentry vehicles for which emissivity is an important parameter. In particular, the TPS must be able to avoid heat goes deep into the vehicle, so as to keep structure safe from the high heat fluxes raised by the aerodynamic heating, so that material properties do not decay because of strains. The metal thermal protection systems (MTPS) are often made of Ni-, Fe-, Co-based alloys, and the surface of Ni, Fe, and Co based alloys used in MTPS involve high frictional heating which can cause surface temperature to rise up to 1000 °C during the flight. Such large heating is undesirable because it can degrade the performance of MTPS<sup>1,2</sup>. To avoid surface heating, a high emissivity coating is applied on MTPS so that heat from the surface can be radiated out during flight<sup>3</sup>.

Apart from that, high emissivity coatings are widely used in many other high temperature applications to effectively transfer the heat by radiation. Increasing demand for energy

and rising energy costs throughout the world has inevitably increased the need for energy users to save or conserve energy, particularly among industrial entities. In many instances, industries that use fired heaters or furnaces, such as refineries and petrochemical complexes, have attempted to maximize fired heater efficiency to thereby reduce fuel consumption. High emissivity coating technology has become a proven means for various high temperature applications to effectively increase radiant heat transfer and save energy without compromising process reliability and safe operation. Specifically, ceramic coatings with high emissivity are applied to the interior of a furnace to improve the efficiency of the furnace which results in energy savings of about 5 per cent - 20 per cent depending on working conditions<sup>4-6</sup>.

Since, loss of effectiveness of these coatings usually occurs as a result of oxidising of the emissivity compound with time, for complete thermal protection of reusable space vehicles, oxidation resistance is required in addition to high emissivity. Advanced metallic TPS utilises a honeycomb structure with thin face sheets that are coated to provide high emissivity, oxidation protection, and low catalytic efficiency. Generally the formulation of a high emissivity composition is attained by mixing a refractory material, a binder and high emissivity additives which include typically a transition metal oxide such as chromium oxide (Cr<sub>2</sub>O<sub>3</sub>), cobalt oxide (CoO<sub>x</sub>), ferrous oxide (Fe<sub>2</sub>O<sub>3</sub>), and nickel oxide (NiO)<sup>7</sup>. A high emissivity coating material composed of carbon was also reported in the literature<sup>4</sup>. Rare earth oxides such as cerium oxide and terbium oxide are also known to be high emissivity agents for industrial applications at very high temperatures<sup>8</sup>. Emissivity coatings using TiC, TiC-Al<sub>2</sub>O<sub>3</sub>-TiO<sub>2</sub>, ZrB<sub>2</sub>, ZrB<sub>2</sub>-MoSi<sub>2</sub> on the niobium

and molybdenum substrates have been reported<sup>9</sup>. Reported emissivity values for TiC, ZrB<sub>2</sub>, and ZrC coatings are: TiC (0.65 to 0.72), ZrB<sub>2</sub> (0.45 to 0.80), and ZrC (0.45 to 0.80) after annealing at 1100 °C temperature<sup>9</sup>. The emissivity value reported for Cr<sub>2</sub>O<sub>3</sub> coating is very high (0.9), but after annealing at 1100 °C decreases to (0.58-0.78) due to the volatilisation of the coating<sup>10</sup>. Recently, the metastable amorphous compound AlPO<sub>4</sub> has been reported for high emissivity applications<sup>11</sup>. This compound has low oxygen diffusivity and no phase transformation at elevated temperatures<sup>11-12</sup>.

Overall, application of thermal protection coating is essential to protect space vehicles from high temperature and ablation of hypervelocity particles as maximum as possible. Moreover, the applied thermal protection coating must provide good oxidation resistance for improving the performance and longevity of the applied coating. Deposition of thermal protection coating can be executed by various techniques like arc evaporation<sup>13</sup>, micro arc oxidation<sup>14-15</sup>, plasma spray<sup>16</sup>, physical vapor deposition<sup>17</sup>, electron beam physical vapor deposition<sup>18</sup>, electrodeposition<sup>19</sup>, pack cementation<sup>20</sup> etc. Deposition of chemical solution on the substrate by dip coating or spray coating followed by curing to develop the coating involves simple processing methodology and allows the deposition of uniform coating over a large area<sup>21-23</sup>.

In the present communication, we report the development of emissivity coating on Ni- based super alloy: Nimonic 75 and C-263, which have numerous aerospace applications since the alloy is lighter and having improved mechanical properties. The development of emissivity coating on these substrates was performed by dip coating as well as by spray coating techniques. Spray coating could be successfully employed to coat larger substrates of any size and has significant improvement over the dip coating technique. Thus, development of high emissivity and oxidation resistant coating on larger substrates by spray coating technique has direct implication in the industrial use of emissivity coating as thermal protection coating and in the metallic TPS in the space vehicles.

## 2. EXPERIMENTALS

### 2.1 Substrate Materials

Ni-base super alloy: Nimonic 75 and C-263 have been used as the substrate materials. The nominal composition (wt %) of Nimonic 75 is 25Cr-5Fe-1Mn-1Si-68Ni and the composition for C-263 is Cr: 19-21%, CO: 19-21%, Mo: 5-6%, Ti: 2.0-2.5%, Fe: 0.7%, B: 0.6%, Mn: 0.4%, Si: 0.4%, Cu: 0.2%, and Ni: 45-50%. Materials were available in the form of 1.5 mm sheets. Samples of sizes 2 cm x 1 cm were cut from these sheets. The surfaces of the substrates were roughened by grit blasting using zircon sand. Subsequently, they were subjected to cleaning in trichloro ethylene, hydrogen peroxide and acetone in that order. The cleaning with each chemical was performed in an ultrasonic cleaner.

### 2.2 Chemical Synthesis of the Aluminum Phosphate Sol

Aluminum phosphate sol was prepared from aluminum nitrate [Al(NO<sub>3</sub>)<sub>3</sub>·9H<sub>2</sub>O] and phosphorous pentoxide (P<sub>2</sub>O<sub>5</sub>) precursors. The details of which have been communicated in

our earlier communication<sup>23</sup>. The synthesised sol was exposed to microwave for 5 min and diluted in ethanol before deposition of coating on C-263 substrate.

### 2.3 Deposition of Coating

For dip coating, grit blasted and cleaned substrates were immersed into the sol at a constant speed of 50 mm/min and allowed to remain in the sol for a minute. It was then withdrawn from the sol at a constant speed of 50 mm/min. In the process, a layer of coating gets deposited on the substrate. After withdrawal the excess liquid was drained out from the surface under gravity and the solvent evaporated leaving behind the coating layers. The dipping and withdrawal of the substrates were performed using a computer interfaced programmable dip coater. The coated substrates were allowed to dry for 10 min in an oven at 120 °C. The dried substrates were then cured at 800 °C in a furnace in air. For achieving higher thickness, the coating steps were repeated after each curing. In such case, the first curing was done at a lower temperature of 500 °C.

For spray coating on larger substrates, aluminum phosphate sol was sprayed to the grit blasted and cleaned substrates using a commercially available sprayer (DeVil Biss, UK, model No. -112GX) followed by their drying and curing.

### 2.4 Emissivity Measurement

Emissivity of the coated surface was measured using Bruker Vertex 80 V spectrophotometer equipped with external emissivity chamber in the wavelength range of 2.5 μm - 25 μm using a black body standard. The instrument measures the reflectivity from which emissivity was calculated following Kirchoff's law of heat transfer by radiation; Emissivity = absorptivity = 1 - reflectivity.

### 2.6 Cyclic Oxidation Study

The uncoated and coated substrates were subjected to cyclic oxidation at 800 °C and 1000 °C for 100 h in air using a box furnace. These temperatures were chosen keeping in mind the high-temperature applications of the emissivity coating. Specimens were cleaned and weighed using a precision balance before oxidation. The specimens were taken out of the furnace after each cycle which corresponds to 10 h of oxidation and cooled to room temperature. After recording their weights, the specimens were put back into the furnace. This procedure was repeated until the completion of 100 h.

### 2.7 Structural Characterisation

X-ray diffraction (XRD) with CuK<sub>α</sub> radiation was utilised for identification of phases in the coating and the oxide layer. Thermal analyses of the dried powder were performed using a TG-DTA analyzer (TA Instruments, SDT 2960) between 30 °C and 1000 °C with a heating rate of 10 °C min<sup>-1</sup> in air. Carbon analysis of the coating material was performed using a LECO gas analyzer (model No. CS444, LECO, USA). The powder samples for TEM observation were prepared by dispersing the powder in methanol and adding a few drops of the suspension on carbon coated TEM grid. A FEI Tecnai 20T TEM was used for observation. The morphology of the coating surface before and after oxidation was characterised

by using a scanning electron microscope (SEM) (ZEISS, UK, model: EVO-18). The SEM was also used for observing the cross-sectional microstructure of the coatings. To determine the coating thickness the coated substrates were sectioned and the sectioned surface was examined by SEM after polishing by standard metallographic technique. The coated substrates were sectioned by mechanical cutter (Isomet-1000) followed by gold sputtering, Ni plating, mounting and standard metallographic polishing as shown in Fig. 1. The presence of elemental C, Al, P, and O were detected with the help of X-ray photoelectron spectroscopy (XPS) measurements with a KRATOS AXIS HS spectrometer (using Al KR radiation). The C 1s (binding energy 285 eV) peak was considered as a reference line for calibration of the energy scale.

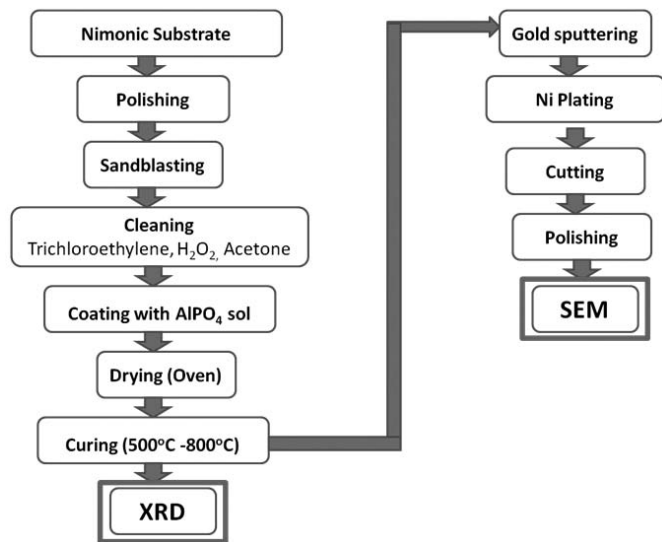


Figure 1. Schematic diagram for substrate preparation, coating, and sample preparation for cross section SEM.

### 3. RESULTS AND DISCUSSION

#### 3.1 Characterisation of the Coating Material

The powder obtained after drying of the precursor sol for high emissivity coating resulted black powder on calcinations at 500 °C - 800 °C in air which comprised  $\text{AlPO}_4$  matrix and graphitised carbon. Thermo gravimetric analysis (TGA) and differential thermal analysis (DTA) measurements were carried out to study the thermal behaviour of the oven-dried powder. The respective DTA -TGA curves are as shown in Fig. 2. The Fig. 2 shows the DTA and TGA curves of the as-dried powder between 25 °C and 1000 °C in air. The TGA shows weight loss in three steps. The initial weight loss of the gel in air between 25 °C and 130 °C is associated with exothermic peak at 85 °C and is attributed to the loss of moisture. The appearance of a sharp exothermic peak at 173 °C in DTA, associated with sharp weight loss between 130 °C and 170 °C in the TGA curve, is due to the ignition of the precursor powder. Above 450 °C there is no further weight loss in the TGA and this suggests that major portion of the carbonaceous materials burn up to 450 °C and the remaining carbonaceous materials in the matrix are stable up to 1000 °C in air. The carbon distributed in the  $\text{AlPO}_4$  matrix imparted black color to the composite. The concentration of carbon present in the 800 °C calcined composite was determined by carbon estimation technique and

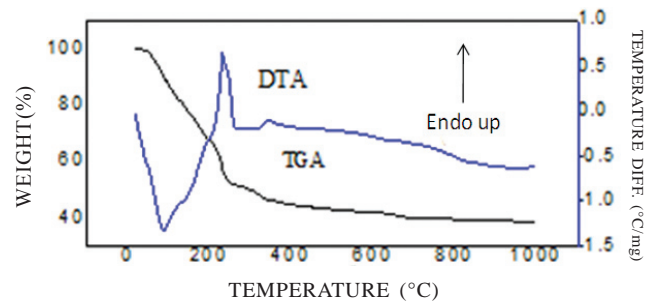


Figure 2. DTA-TGA curves for oven dried powder obtained from the precursor sol.

was found to be ~5 weight %. The presence of carbon was also confirmed by Raman spectroscopy. Raman spectroscopy was performed on  $\text{AlPO}_4\text{-C}$  composite powder calcined at 500 °C – 900 °C in air and it was observed that all the calcined samples showed peaks for carbon in Raman spectra. Figure 3 (a) and (b) show the Raman spectra of the  $\text{AlPO}_4\text{-C}$  composite powder calcined at 700 °C and 900 °C, respectively. The peaks at 1345  $\text{cm}^{-1}$  and 1600  $\text{cm}^{-1}$  can be attributed to the presence of carbon as reported earlier in literature for graphite by Yan Wang<sup>24</sup>, *et al.* and F. Tuinstra<sup>25</sup>, *et al.* The presence of the elements: Al, P, O and C in the  $\text{AlPO}_4\text{-C}$  composite powder were detected by XPS spectroscopy. Figure 4 shows the XPS spectra of the composite. The spectra indicates the presence of Al(2p), P(2p), C(1s), and O(1s), confirming that the coating material is actually a composite comprises of  $\text{AlPO}_4$  and carbon. It is to be noted that the source of carbon is attributed to the alcohol used during synthesis of the precursor sol. No carbonaceous material other than the alcoholic solvent was added in the precursor chemicals. In this composite, the  $\text{AlPO}_4$  matrix is nearly amorphous and retains its amorphous nature up to very high temperature and carbon in the matrix was protected from the oxidation up to 1000 °C due to extremely low oxygen diffusivity in the nearly amorphous  $\text{AlPO}_4$  based matrix.

Scanning of the 900 °C calcined  $\text{AlPO}_4\text{-C}$  composite powder by SEM with very high magnification showed the presence of nano grains of hexagonal carbon distributed in  $\text{AlPO}_4$  matrix (Fig. 5(a)). The figure given in the inset revealed

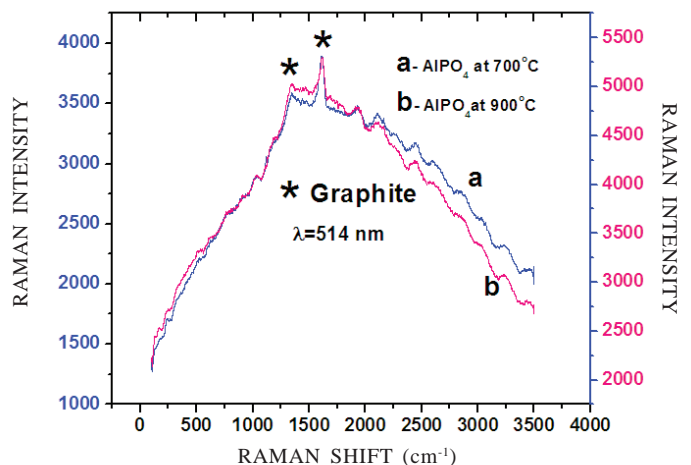


Figure 3. Raman spectra of the  $\text{AlPO}_4\text{-C}$  composite powder calcined at (a) 700 °C and (b) 900 °C.

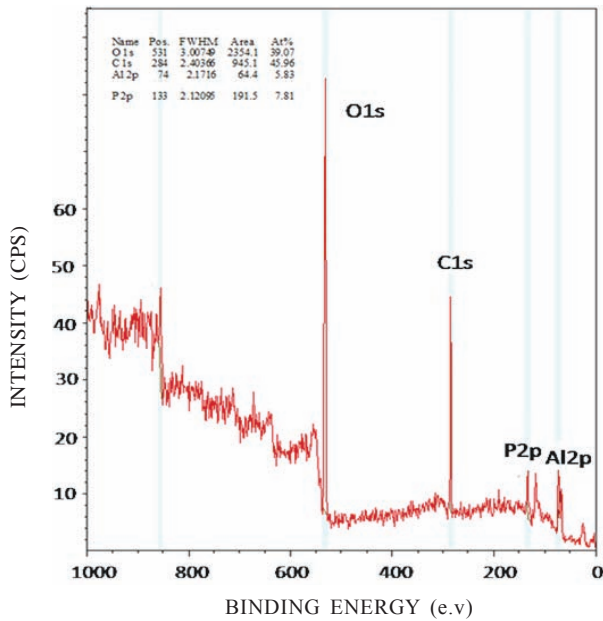


Figure 4. XPS spectra of the  $\text{AlPO}_4\text{-C}$  composite powder showing the peaks for Al(2p), P(2p), C(1s), and O(1s) at 74.8, 134, 285, and 532 eV, respectively.

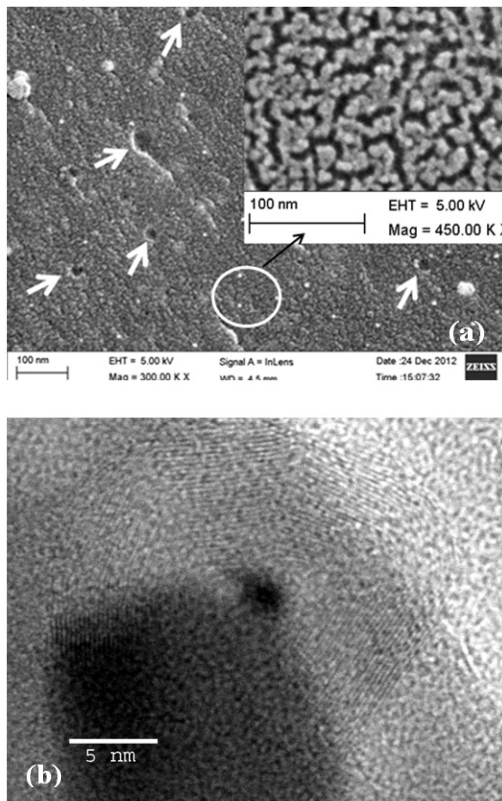


Figure 5. (a) Nanostructure of coating material at very high magnification (300000X) (hexagonal graphitised carbons distributed in the  $\text{AlPO}_4$  matrix are indicated by arrows) and inset shows nanostructure of the matrix at 450000 magnification) and (b) high resolution TEM micrograph of the 900 °C calcined  $\text{AlPO}_4\text{-C}$  composite powder revealing the presence of nano carbon with hexagonal symmetry, in the nearly amorphous  $\text{AlPO}_4$  matrix.

the matrix is constituted of 2-5 nm sized  $\text{AlPO}_4$  grains. Figure 5(b) shows high resolution TEM micrograph of the same powder revealing the presence of nano carbon with hexagonal symmetry, in the  $\text{AlPO}_4$  matrix.

### 3.2 Characterisation of the Dip Coated and Spray Coated Substrates

#### 3.2.1 Characterisation by SEM and Polarised Light Microscopy

High emissivity coating based on amorphous  $\text{AlPO}_4\text{-C}$  composite was applied on C-263 substrate by dip coating of the substrate in the chemical precursor sol followed by curing at high temperatures as mentioned in the experimental section. The coating, in general, appeared black in colour and showed no visual cracking or delamination. The surface morphologies of the 5-layer coating were analysed by SEM and are presented in Fig. 6(a). The surface of the 5-layer coating shows cracking in the thicker deposit layers. This type of cracking has been reported in yttrium stabilised zirconia ceramic coating deposited on metallic substrate by sol-gel dip coating<sup>26</sup>. It is believed that such cracking is caused due to the uneven shrinkage resulted from quick densification of the coating material present in the

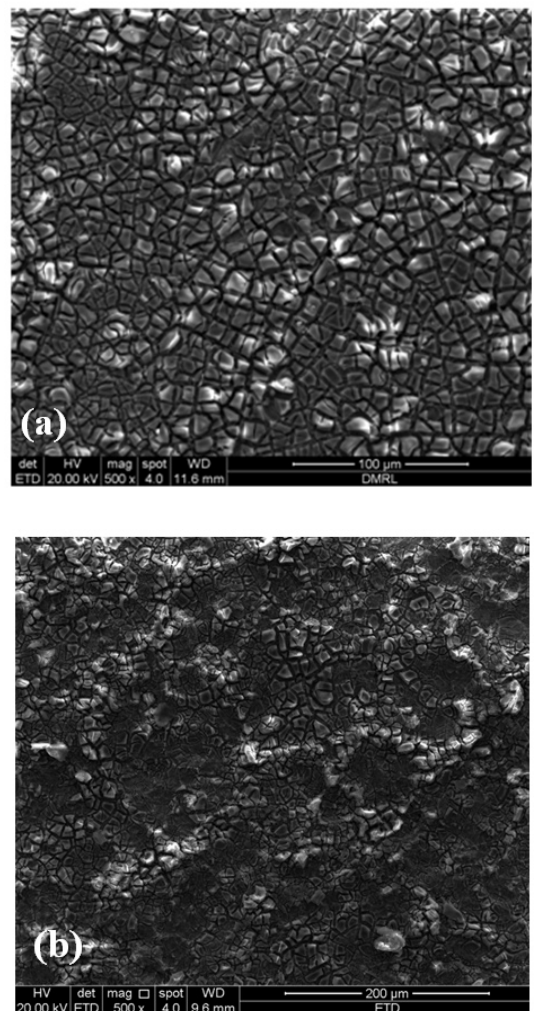


Figure 6. SEM micrographs of the (a) dip-coated and (b) spray-coated C-263 substrates showing the surface morphology of the coated substrates.

thicker layer accompanied by the removal of alcoholic solvents during thermal treatment. Since the coating is adhered to the substrate and cannot shrink in the direction parallel to the substrate surface, it leads to cracking in the coating layers.

The surface morphology of the spray coated substrate is similar to that of the dip coated substrate (Fig. 6(b)). Despite the presence of cracks, the coated materials on both the dip coated and spray coated substrates were found to be sufficiently adherent to the substrates and the coated substrates were easy to handle after curing.

Figure 7(a) shows the digital photographs of the bare and dip-coated substrates. Feasibility of applying the high emissivity coating by spray coating technique was experimented by spraying the 'AlPO<sub>4</sub>-chemical sol' on larger C-263 substrates using commercially available spray gun as stated in the experimental section followed by drying and curing. It was observed that emissivity coating could be successfully applied on different grit blasted larger substrates by standard spray coating technique. Figure 7(b) shows the digital photographs of the coated and cured C-263 substrate of size ~ 30 cm X 20 cm. Figure 7(c) shows coated and cured honeycomb TPS panel of size ~ 35 cm x 20 cm made from C-263 alloy plate.

Coating thickness of the dip coated substrates is determined by observing the cross-sectional view in SEM (Fig. 8 (a) and (b)). Whereas, coating thickness of the spray coated substrates is determined by observing the cross-sectional view

in polarised light microscopy (Fig. 8 (c) and (d)). Thicknesses of the multilayer coatings are listed in Table 1. As expected, the thickness of the coatings increased with increase in the number of layer. It has been observed from the micrographs that uniformity in thickness in the dip coated substrates is more than that in spray coated substrates.

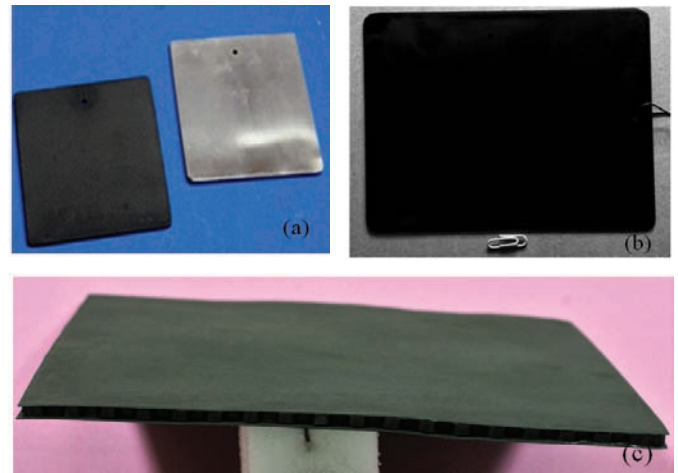


**Figure 7.** Digital photographs of the bare substrate (6 cm x 6 cm) and dip-coated substrate by the aluminum phosphate chemical sol (b) spray-coated C-263 substrate of size ~ 30 cm x 25 cm (c) spray-coated C-263 honeycomb TPS panel of size ~ 35 cm x 20 cm.

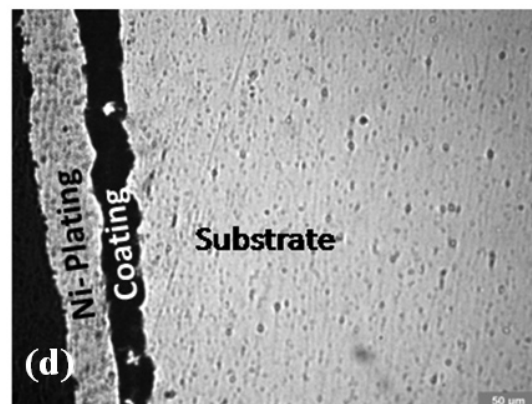
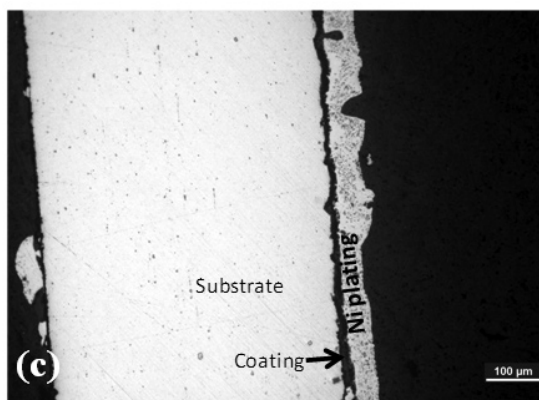
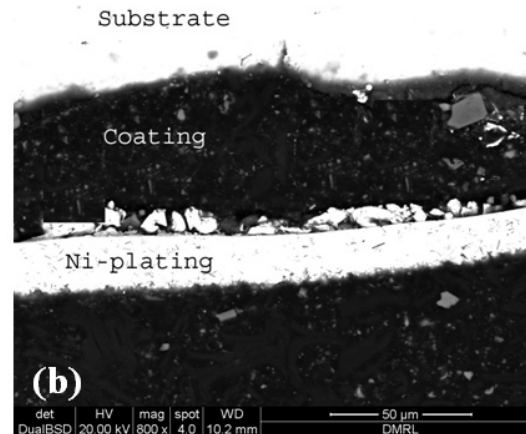
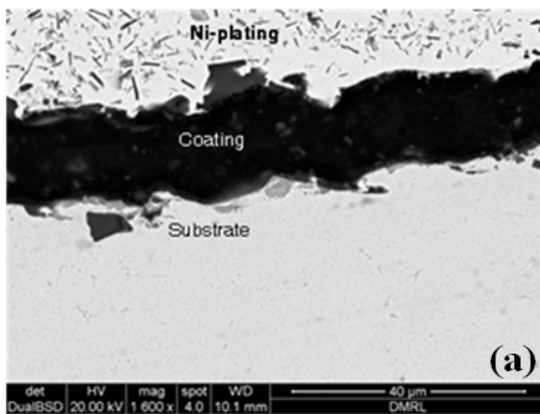


**Figure 8.** SEM micrographs of the cross-section of the dip-coated and cured substrates (a) 3-layer dip coating (b) 5-layer dip coating and optical micrographs of the cross-section of the spray-coated and cured substrates (c) 3-layer spray-coating and (d) 5-layer spray-coating showing the coating thickness.

**Table 1. Measured emissivity and coating thickness for the multilayered dip coated and spray coated substrates.**

No. of the coating layers	Thickness of the coating ( $\mu\text{m}$ )	Emissivity ( $\epsilon$ )	Weight gain of the substrate after coating and curing ( $\text{mg}/\text{cm}^2$ )
1- dip coating	5-7	0.65-0.7	1.2-1.4
3- dip coating	17-23	0.85-0.88	3.4-3.6
5- dip coating	35-42	0.89-0.91	5.5-6.0
3- spray coating	15-22	0.80-0.83	3.2-3.4
5- spray coating	30-40	0.83-0.86	5.0-5.5

### 3.2.2 Characterisation of the Dip Coated and Spray Coated Substrates for Emissivity

Characterisation of emissivity was performed on the coated substrates as mentioned in the experimental section. The instrument measures reflectivity at variable wavelength.

Absorptivity ( $\alpha$ ) is material property which describes the capability of a material to absorb electromagnetic radiation and having a quantitative value between 0 and unity. According to Kirchhoff's second law<sup>27</sup>:

$$\alpha = \epsilon \quad (1)$$

where  $\epsilon$  is emissivity of the material.

The energy conservation law correlates three different optical properties of a material:

$$\epsilon + \tau + \rho = 1 \quad (2)$$

where  $\tau$  and  $\rho$  are the coefficients of transmission and reflection(reflectivity) respectively.

For opaque coatings  $\tau \sim 0$ , and hence

$$\epsilon = 1 - \rho \quad (3)$$

i.e. for opaque coatings emissivity=1-reflectivity.

The results of the emissivity measurements in the wavelength range:  $2 \mu\text{m} - 25 \mu\text{m}$  for the dip coated substrates are shown in the plotted graphs (Fig. 9(a)). From the graph it is observed that distribution of radiative energy over the wave length range  $2 \mu\text{m} - 25 \mu\text{m}$  remains almost unchanged with the variation of coating thickness. However, decrease in fluctuation of emissivity with increasing coating thickness in the wave length range  $7 \mu\text{m} - 12 \mu\text{m}$  is observed (Fig. 9(a)). Emissivity of the 3-layered and 5-layered coated substrates is varying in the range: 0.7-0.9 in the wavelength range: 1-7 micron and remains around 0.9 for the rest of the wave length:  $7 \mu\text{m} - 25 \mu\text{m}$  (Fig. 9(a)). The emissivity of the 1-layer coating is considerably lower. The average emissivity values for 1-layer, 3-layer, and 5-layer coatings are calculated by taking the average of the emissivity values for the entire wavelength range:  $2 \mu\text{m} - 25 \mu\text{m}$ . The calculated average emissivity values for the dip coated substrates are given in Table 1. The variation of emissivity with wave length for the spray coated substrate is similar to that for the dip coated substrates. However, the spray coated substrates offered little lower emissivity than the dip coated substrates (Fig. 9(b)).

### 3.3 Cyclic Oxidation Studies on the Coated and Bare Substrates

High temperature oxidation resistance of the coated substrates is an important criterion for their survival in actual application. The applied thermal protection coating

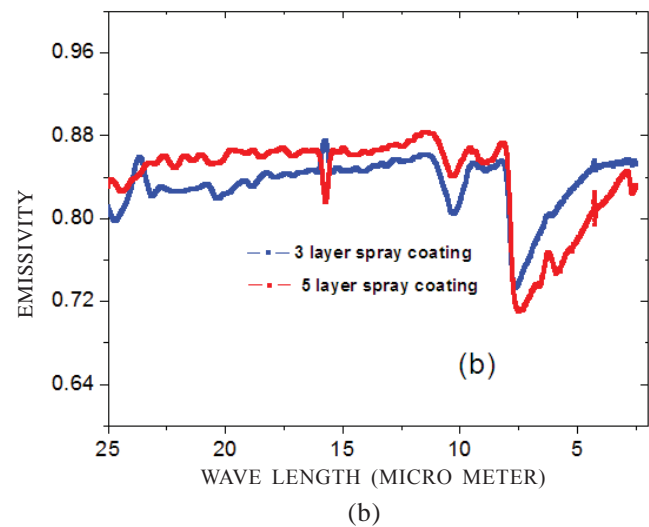
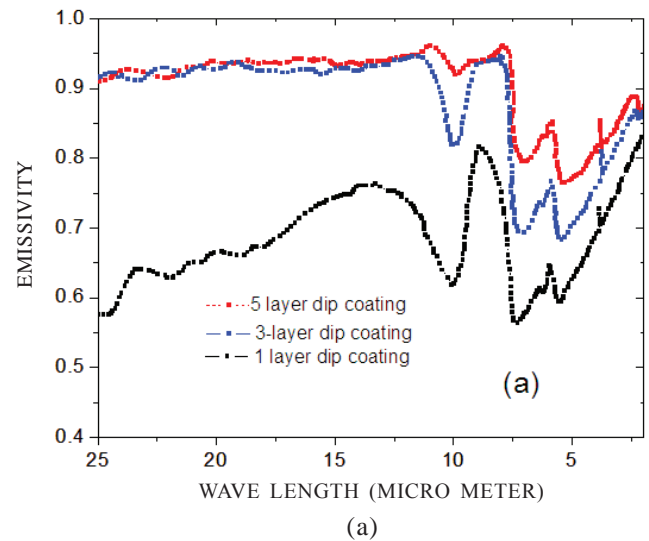


**Figure 9. Variation of emissivity with wave length of the (a) dip coated substrates, and (b) spray coated substrates.**

must provide good oxidation resistance for improving the performance and longevity of the space vehicle. In the present work, the oxygen diffusivity in the coated material i.e. amorphous  $\text{AlPO}_4$  is extremely low and the coating imparts high oxidation resistance to the substrate in addition to high emissivity. The oxidation resistance of the coated material was checked by heating a coated and bare substrate at  $800 \text{ }^\circ\text{C}$  for 1 h in air.

The XRD results of the heat treated coated and bare substrates are shown in Fig. 10. XRD of the heat treated bare substrate shows the lines of  $\text{Cr}_2\text{O}_3$  and  $\text{MoO}_3$  with considerable intensity. The intensity of these lines is much lower in the XRD pattern of heat treated coated substrate. The results of these experiments signify that amorphous  $\text{AlPO}_4$  coating imparts considerable oxidation resistance to the substrate.

To evaluate the oxidation resistance of the coated C-263 substrates at higher temperatures, cyclic oxidation studies were performed. For this purpose the coated and bare substrates were exposed to high temperatures for 10 consecutive cycles (1 cycles=10 h) as stated in the experimental section. Since the emissivity increased with increasing the number of coating

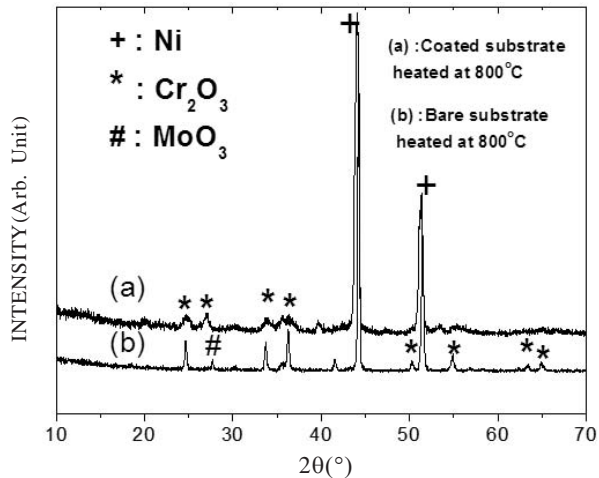


**Figure 10.** XRD results of the coated and bare substrates after heat treatment at 800 °C for 1 h in air.

layers and gets saturated with 5-layer coating, substrates with 5-layer layer coating have been evaluated for oxidation resistance. Figure 11 shows the change in weight of the coated and bare C-263 substrates due to oxidation with the exposure at 800 °C and 1000 °C in air for different duration. The coated substrate showed very low weight change throughout the full oxidation cycling (100 h) signifying minimum oxidation of the coated substrate (Fig. 11(b) and (d)). In contrast, the bare substrate showed substantial weight changes over the whole period of cyclic oxidation (11(a) and (c)). Moreover, the bare substrate underwent spallation multiple number of times which are reflected in the weight change curves at both the temperatures (800 °C and 1000 °C). Spallation in any step of cyclic oxidation can be characterised by sudden weight loss which follows the ‘oxidation- weight gain’ in the previous steps. This happens because thick oxide layer resulted from the progressive oxidation of the bare substrate gets separated from the parent substrate after gaining sufficient weight. From the figure it is observed that for the bare substrates spallation occurred multiple times (3<sup>rd</sup>, 5<sup>th</sup>, and 9<sup>th</sup> cycle in Fig. 11(a); 2<sup>nd</sup> cycle in Fig. 11(c)) during total 100 h of cyclic thermal exposure.

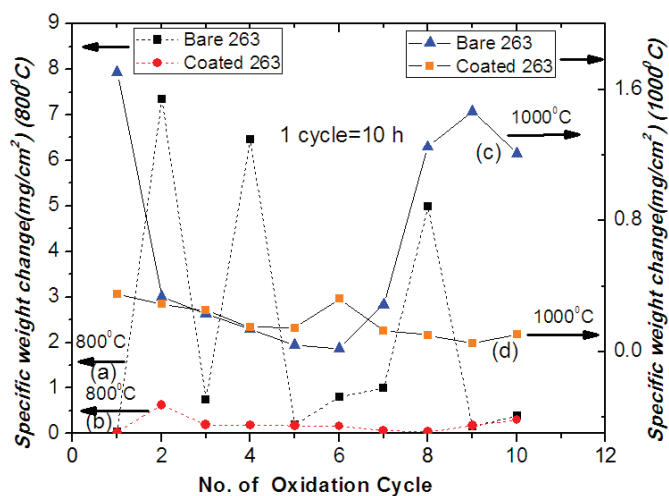


**Figure 11.** Cyclic oxidation test of the (a) bare substrate, 800 °C and (b) coated substrate, 800 °C (c) bare substrate, 1000 °C and (d) coated substrate, 1000 °C.

#### 4. CONCLUSION

Aluminum phosphate based high emissivity coating was applied on C-263 substrate by dip coating and spray coating technique followed by curing of the green coating. The coating material is black in colour and is a composite of AlPO<sub>4</sub> and carbon. The coating exhibited a reasonably good adhesion with the substrate. Presence of carbon in the matrix of the coated material was detected by SEM, TEM, and XPS analyses and carbon imparted high emissivity to the coating. The amount of carbon in the composite was found to be ~ 5 weight per cent. The coating exhibited high emissivity varying from 0.6 to 0.9 in the wave length range: 2 μm - 25 μm depending on the thickness of the multilayered coating. Emissivity increased with increasing the thickness of the coating. Larger substrates and TPS panels could be successfully coated by spray coating technique. Emissivity offered by the spray coated substrates were little lower than that of the dip-coated substrates. Apart from high emissivity, coated substrates showed good oxidation resistance compared to the bare substrate, in air which was confirmed by cyclic oxidation experiment at both 800 °C and 1000 °C over 100 h of thermal exposure.

#### REFERENCES

- Falz, M. & Leonhardt, M.G. PVD coatings with high IR emissivity for high temperature applications of Co based alloys. *Surf. Coat. Tech.*, 1993, **61**(1-3), p-97.
- He, X.; Li, Y.; wang, L.; Sun, Y. & Zhang, S. High emissivity coatings for high temperature application progress and prospect. *Thin Solid Film*, 2009, **517**, 5120-5129. doi: 10.1016/j.tsf.2009.03.175
- Laub, B. & Venkatapathy, E. Thermal protection system technology and facility needs for demanding future planetary missions. International Workshop on Planetary Probe Atmospheric Entry and Descent Trajectory Analysis and Science, Lisbon, Portugal, 6-9 October 2003.
- Yu, Jun S.; Sung, Jae H.; Park, S. & Lee, J.C. Emissive carbon coating for energy saving. *Materials Science Forum*, 2005, **486-487**. pp 666-669. doi: 10.4028/www.scientific.net/MSF.486-487.666
- Xin, X. & Qingchang, G. and Yi, J. High emissivity refractory coating improves furnace output in china. *Industrial Heating*, 1999, **66**, p. 49
- Geraldine, J. Heynderickx & Masatsugu, Nozawa. High-emissivity coatings on reactor tubes and furnace walls in steam cracking furnaces' *Chemical Engineering Science* 2004, **59**, 5657 – 5662.
- Xudong, Cheng; Wei, Duan; Wu, Chen; Weiping, Ye; Fang, Mao; Fei, Ye & Oi. Zhang. Infrared radiation coatings fabricated by plasma spray. *J. Thermal Spray Tech.*, 2009, **18**(3) 448-450.
- Holcombe, Cressie E., Jr. & Chapman, Lloyd R. High emissivity coating composition and method of use. U.S. patent No. 6007873,
- Cockeram, B.V.; Measures, D.P. & Mueller, A.J. The development and testing of emissivity enhancement coatings for thermophotovoltaic (TPV) radiator applications. *Thin Solid Film*, 1999, **355**(1), 17-25.

- doi: 10.1016/S0040-6090(99)00438-1
10. Burford, R.A. & Fowler, J.B. Ceramic, Black-Body, high emissivity coatings for improved efficiency of fired heaters. *Heat Resistant Materials II*, ASM Intl., Materials Park, OH, 1995, 453-456.
  11. Sankar, S. & Steiner Kimberly A. Aluminum phosphate compounds, compositions, materials and related composites. U.S. patent No. 7682700, March 2010.
  12. Sankar, S. & Steiner Kimberly A. High temperature amorphous composition based on aluminum phosphate. U.S. patent No. 6461415, October 2002.
  13. Koller, C.M.; Hollerweger, R.; Sabitzer, C.; Rachbauer, R.; Koložsvári, S.; Paulitsch, J. & Mayrhofer, P.H. Thermal stability and oxidation resistance of arc evaporated TiAlN, TaAlN, TiAlTaN, and TiAlN/TaAlN coatings. *Surf. Coat. Technol.*, 2014, **259**, Part C, 599–607.  
doi: 10.1016/j.surfcoat.2014.10.024
  14. Li, Sizhen; Bai, Jingying; Feng, Li; Zhang, Ligong; Cui, Qingxin; Jiang, Wenwu & Zhao, Guimei. Research on micro-arc oxidation coatings with thermal control on magnesium Alloy. *Physics Procedia*, 2013, **50**, 185–190.  
doi: 10.1016/j.phpro.2013.11.030
  15. Dudareva, N.Yu.; Kalschikov, R.V.; Butusov, I.A.; Grin, R.R.; Alexandrov, I.V. & Musin, F.F. The investigation of the effect of micro-arc oxidation modes on the adhesion strength of coatings. *J. Eng. Sc. Tech. Review.*, 2014, **7**(5) 5-8.
  16. Pourbafrani, M.; Razavi, R. Shoja; Bakhshi, S.R.; Loghman-Estarki, M.R. & Jamali, H. Effect of microstructure and phase of nanostructured YSZ thermal barrier coatings on its thermal shock behavior. *Surface Engineering*, 2015, **31**(1) 64-73.  
doi: 10.1179/1743294414Y.0000000397
  17. Merl, D. Kek; Panjan, P. & Milošev, I. Effect of tungsten content on properties of PVD sputtered Al–WX alloys. *Surface Engineering*, 2013, **29**(4) 64-73.
  18. Hosseini, S.H.; Mirdamadi, S. & Rastegari, S. Investigating efficiency of  $\alpha$ -Al<sub>2</sub>O<sub>3</sub> diffusion barrier layer in oxidation of EB-PVD NiCrAlY coatings. *Surface Engineering*, 2015, **31**(2) 146-155.  
doi: 10.1179/1743294414Y.0000000365
  19. Shamsolhodaei, A.; Rahmani, H. & Rastegari, S. Effects of electro deposition parameters on morphology and properties of Zn–TiO<sub>2</sub> composite coating. *Surface Engineering*, 2013, **29**(9) 695-699.  
doi: 10.1179/1743294413Y.0000000197
  20. Li, Yang; Zhou, Wei; Xiao, Peng; Luo, Heng; Wen, Zhongliu & Luo, Wei. The anti-oxidation behavior and infrared emissivity property of SiC/ZrSiO<sub>4</sub>-SiO<sub>2</sub> coating. *J. Mater. Sci.: Mat. Electr.*, 2014, **25**(12), 5433-5440.  
doi: 10.1007/s10854-014-2325-0
  21. Tian, H.; Wang, Y.M.; Guo, L.X.; Ouyang, J.H.; Zhou, Y. & Jia, D.C. Oxidation resistance of SiO<sub>2</sub> bonded coating formed on Ti–Al–Zr alloy. *Surface Engineering*, 2014, **30**(3) 204-211.  
doi: 10.1179/1743294413Y.0000000241
  22. Liu, R. & Shi, L. Formation of t'-YSZ nanocoating from composite sols. *Surface Engineering*, 2013, **29**(9) 700-702.  
doi: 10.1179/1743294413Y.0000000187
  23. Roy, S.; Maharana, R.; Laxmi, S. Gokul; Sakthivel, Y.; Roy, Manish; Bhanu Prasad, V.V. & Das, D. K. AlPO<sub>4</sub>–C composite coating for high emissivity and oxidation protection applications. *Surface Engineering*, 2013, **29**(5) 360-365.  
doi: 10.1179/1743294413Y.0000000119
  24. Wang, Yan; Alsmeyer, Daniel C. & Mc Creery, Richard L. Raman spectroscopy of carbon materials: structural basis of observed spectra. *Chem. Mater.*, 1990, **2**, 557-563.  
doi: 10.1021/cm00011a018
  25. Tuinstra F. & Koenig, J.L. Raman Spectrum of Graphite. *J. Chemical Phys.*, 1970, **53**(3) 1126.  
doi: 10.1063/1.1674108
  26. Barrow, D.A.; Petroff, T.E. & Sayer, M. Thick ceramic coatings using a sol-gel based ceramic-ceramic 0-3 composite. *Surf. Coat. Technol.*, 1995, **76–77**, 113.  
doi: 10.1016/0257-8972(95)02562-6
  27. Seronde, F.; Echehut, P.; Coutures J. P. and Gervais, F. A microscopic approach to glass coatings. *Mater. Sc. Eng.*, 1991, (B8) 315-327.

#### ACKNOWLEDGEMENT

The authors thankfully acknowledge the financial support from the Defence Research Development Organisation, Ministry of Defence, New Delhi, for carrying out the present work. Authors are thankful to Director, DMRL for giving permission for carrying out the research work. The authors would like to thank Dr S. Mahajan, Project Advisor; Dr S.S. Prasad, Project Leader, and Dr T. Raghu for their constant encouragement and helpful discussion. The authors also wish to thank Dr P. Ghosal, Dr A.K. Singh, Scientists of DMRL, and Dr Pradip Paik, Professor, Central University, Hyderabad, for their help in SEM, XRD, and TEM, respectively.

#### CONTRIBUTORS

**Dr Subir Kumar Roy** obtained his PhD from, Indian Institute of Technology, Kharagpur and presently working as Scientist 'E' in DMRL, DRDO, Hyderabad. At DMRL, Hyderabad, Dr. Roy is working in the area of high emissivity and oxidation resistant coating for high temperature applications. He is also involved in the research and development activity on ferroelectric materials in the form of bulk as well as thin films. Dr. Roy has around 35 papers in the national and international Journals to his credit.

**Mr S. Rangaswamy Reddy** has obtained Masters in Inorganic Chemistry from Osmania University. He has been working as Junior Research Fellow in DMRL since 2014. His research activities include development of high emissivity coating and Ferroelectric bulk and thin film materials.

**Dr V.V. Bhanu Prasad** obtained his PhD in Powder Metallurgy from the Indian Institute of Technology (IIT) Bombay. He is presently working as Scientist 'G' at the Defence Metallurgical Research Laboratory (DMRL), Hyderabad. He heads the Ceramics and Composites Group and works in the area of development of various types of ceramics and ceramic matrix composites for



defence applications. He is a recipient of the Andhra Pradesh Scientist Award in the Year 2005 and DMRL Technology Group Award (as team leader) in 2010. He has more than 75 research papers and technical publications to his credit. His research interests are in the area of Aluminium and Titanium Matrix composites, Reaction Bonded Silicon Carbide (RBSC) and Boron carbide (RBBC), synthesis and consolidation of Ultra High Temperature Ceramics (UHTCs), Cf-C-SiC & Cf-SiC composites and electro ceramics for defence applications.

**Ms P. Sindhuja** obtained her MSc (Physics) from Thiagrajar College of Engineering, Madurai, in 2013. She successfully completed her MSC project work on High emissivity coating for high temperature applications in DMRL in the year 2013 and presently working in a reputed industrial organisation in Tamilnadu, India.

**Dr Dipak Das** received PhD (Metallurgical Eng.) from B.H.U. Varanasi in 2001. He is working as a Scientist 'G' in Defence Metallurgical Research Laboratory (DMRL), Hyderabad. Research areas: High temperature coatings, thermal barrier coatings, diffusion coatings, coatings for hypersonic applications, laser processing of materials.